RESEARCH PAPER

IN SILICO DRUG DISCOVERY APPROACH USING PLANT-DERIVED COMPOUNDS FOR THE MANAGEMENT OF POLYCYSTIC OVARIAN DISEASE TARGETING HUMAN PLACENTAL AROMATASE CYTOCHROME P450 (CYP19A1)

Chitra Devi. T[1]*, Kavinprakash. T[2], Saniya. P[2], Madhubalan. V[2]
[1]Assistant Professor, Department of Biotechnology, Bannari Amman Institute of Technology, Sathyamangalam – 638401, Erode
[2]Department of Biotechnology, KIT-Kalaignarkarunanidhi Institute of Technology, Coimbatore - 641 402, India
*Corresponding author: chitrapkrs@gmail.com Orcid ID: 0000-0002-0056-7168

ABSTRACT
Polycystic Ovarian Disease (PCOD) is an endocrine disorder of women that causes hormonal and metabolic imbalance. Aromatase (CYP19A1) is known drug target for the correction of hormonal imbalance in PCOD as it is the rate controlling enzyme in the steroid pathway for the conversion of androgens to estrogens. In the present study, an integrated in silico screening protocol was employed to identify the potent plant derived CYP19A1 inhibitors through molecular docking, molecular dynamics simulation and ADMET profiling. The compounds that effectively bind to the active site of CYP19A1 (PDB ID: 5JL6) were identified by docking of over 500 phytocompounds using Auto Dock Vina in PyRx. The compound which exhibited highest binding affinity was subject to 100 ns MD simulation using GROMACS with CHARMM36 force field. The pharmacokinetic and toxicity profiles of the shortlisted compounds were determined using Swiss-ADME and Pro Tox-3, respectively. The list of compounds used for docking were ranked based on the CYP19A1 binding affinity and Deserpidine was identified as the molecule of highest binding affinity (10.2 kcal/mol) which formed interactions with all the amino acids present within the androstenedione binding site of CYP19A1. The stability of Deserpidine-CYP19A1 complex formed during docking was further validated by MD simulation and the trajectory parameters such as RMSD (0.22-0.45 nm), radius of gyration (2.27-2.31 nm) and per-residue RMSF remained stable throughout the simulation. Deserpidine had high predicted gastrointestinal absorption along with low toxicity. In conclusion, Deserpidine appears to be a potential natural CYP19A1 inhibitor with good pharmacokinetic characteristics and confirmed experimental validation for PCOD management is recommend.

Keywords: *Aromatase Inhibition; CYP19A1; Deserpidine; PCOD; Molecular Docking; Molecular Dynamics; Phytochemicals; Computational Drug Design; Estrogen Biosynthesis.*
How to cite this article: Chitra Devi. T1* Kavinprakash. T2 Saniya. P2 Madhubalan. V2. IN SILICO DRUG DISCOVERY APPROACH USING PLANT-DERIVED COMPOUNDS FOR THE MANAGEMENT OF POLYCYSTIC OVARIAN DISEASE TARGETING HUMAN PLACENTAL AROMATASE CYTOCHROME P450 (CYP19A1). Int J Drug Deliv Technol. 2026;16(89s):286-292. DOI: 10.25258/ijddt.16.89s.29.

1. INTRODUCTION

PCOD which is the most common endocrine disorder in women of reproductive age, with an estimated prevalence of 8–13% among women of reproductive age and 4–7% among general population[1,2]. PCOD has 3 clinical features, hyperandrogenism, oligoanovulation and polycystic ovaries, with insulin resistance, dyslipidaemia and low-grade of chronic inflammation3. It is also reported that women with PCOD are associated with the risk to develop metabolic syndrome, T2DM, CVD and endometrial carcinoma[1]. Biosynthesis of estrogen is abnormal in PCOD One study has hypothesized that aromatase cytochrome P450 activity, which is controlled by the CYP19A1 gene, may be abnormal in women with PCOD[4]. Aromatase cytochrome P450 is a cytochrome P450 enzyme that irreversibly aromatizes the C19 androgens [androstenedione and testosterone] into C18 estrogen[estrogen], and is the rate limiting enzyme in the biosynthesis of the estrogen[4]. Aromatase cytochrome P450 activity is lower in the ovarian granulose cells of women with PCOD4, and this may be one of the causes for the accumulation of the androgen and the inability of the androgen to suppress serum estradiol levels by the hypothalamo-pituitary axis[4,5]

Various polymorphisms in CYP19A1 gene have been described in women with PCOS, directly associating CYP19A1 mutation with the pathogenesis of the condition[5]. The pharmacological treatments of PCOD are based on combined oral contraceptives, anti-androgens, and insulin sensitisers such as metformin. Although these agents are valid for treatment of the symptoms, their chronic use may be associated with side effects, and they do not directly regulate the enzymatic processes responsible for the existing disruption of the steroidogenic axis[1]. The absence of effective medical treatments has led to the continuous study of phytochemicals as possible treatments for PCOD that could act simultaneously on multiple pathways, have a good safety profile, and be mechanistically

relevant[6,7]. Bioactive components of plant origin like flavonoids, polyphenols, and alkaloids have been observed to regulate the activity of steroidogenic enzymes and restore metabolic alterations in PCOD models[7,8]. Inhibition of hyperandrogenism by phytoconstituents of *Asparagus racemosus* has been demonstrated by in vitro/in silico studies[9] and also artemisinin derivatives have been found to improve polycystic ovarian syndrome by modulating CYP11A1-catalysed steroidogenesis.[10]. Non-polar phytocomponents of aloe vera have similarly shown promise in the management of ovarian function in PCOS[8]. Inositol, a naturally occurring signalling molecule, has been extensively studied for improving insulin sensitivity and restoring ovulatory function in PCOD[11]. The application of computational drug discovery methods including molecular docking, virtual screening, and molecular dynamics simulation has transformed the early stages of drug development by enabling rapid, cost-effective identification and prioritization of candidate compounds before resource-intensive experimental testing[12]. In silico approaches have been employed with increasing frequency in the context of PCOD to screen phytochemical libraries against validated molecular targets, including CYP19A1[12]. The current work uses a comprehensive in silico workflow to screen more than 500 plant-origin compounds in the crystal structure of human placental aromatase CYP19A1 (PDB ID: 5JL6). Molecular docking, 100 ns MD simulation along with multi-endpoint ADMET predictions have been used to screen, as well as find the lead compounds with high likelihood of CYP19A1 inhibition for PCOD.

2. MATERIALS AND METHODS

2.1 Protein Target Preparation

The human placental aromatase CYP19A1 crystal structure in complex with androstenedione (PDB ID 5JL6; resolution: 2.75 Å) was downloaded from the RCSB Protein Data Bank (PDB). Protein preparation was performed in Auto Dock Tools 1.5.6. Water molecules present in the crystal structure were removed, as were all heteroatoms, and the remaining atom types were assigned atom types and Gasteiger partial charges. Polar hydrogen atoms were added to the remaining atom types and energy minimization was performed to remove steric overlaps and optimize the 3D structure of the protein. The active site was defined by the binding coordinates of the co-crystallized androstenedione ligand to ensure biologically relevant docking orientations.

To validate the docking protocol, the co-crystallized androstenedione was extracted and re-docked into the prepared receptor. An RMSD of less than 2.0 Å between the re-docked and crystallographic poses was applied as the acceptance criterion, confirming the reliability of the docking parameters before proceeding with library screening.

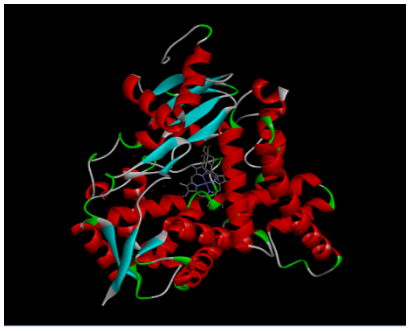


Figure 1. Three-dimensional crystal structure of human placental aromatase CYP19A1 (PDB ID: 5JL6) co-crystallized with androstenedione (shown in stick representation). The active site cavity is highlighted.

2.2 Ligand Library Preparation

A curated library of over 500 plant-derived bioactive compounds was assembled from established phytochemical databases including the IMPPAT database (Indian Medicinal Plants, Phytochemistry and Therapeutics), Dr. Duke's Phytochemical and Ethnobotanical Databases, and the ZINC Natural Products subset. Three-dimensional structures were retrieved in SDF format. Each compound was subjected to energy minimization using the Universal Force Field (UFF) in Open Babel 3.1.1 to achieve a stable low-energy conformation. The flexible rotatable bonds were determined and defined as such to allow conformational sampling during docking. All of the ligand files were converted to PDBQT format using Auto Dock Tools in preparation for Auto Dock Vina.

2.3 Molecular Docking

Virtual screening was carried out using Auto Dock Vina (PyRx 0.8). The grid box was placed on the androstenedione binding pocket of CYP19A1 with a volume of 25 × 25 × 25 Å and grid spacing of 0.375 Å. Each ligand was docked separately with an exhaustiveness of 8 and produced up to 9 binding modes. All 500+ compounds were ranked by their lowest predicted binding free energy (kcal/mol). Top-ranked compounds were prioritized based on binding affinity, interaction profile with key active-site residues, and drug-likeness. The lead compound was selected for subsequent MD simulation and ADMET analysis. Docked poses and protein–ligand interactions were visualized using Discovery Studio Visualizer 2021.

2.4 Molecular Dynamics Simulation

To check the stability of complex (lead protein-ligand) under physiological condition, 100 ns MD simulation was carried out in GROMACS 2022.3 using CHARMM36 force field. The topology of proteins was built by CHARMM36 force field parameters. The topology and force field parameter for Deserpidine was built using CHARMM General Force Field (CGenFF) server. The complex was solvation in cubic box with explicit TIP3P water molecules, where at least 1.0 nm distance between the surface of the protein molecule and the box wall

was considered. Sodium and chloride counter-ions were added to cancel the charge of the system and to maintain a salt concentration of 0.15 M NaCl.
Minimize energy using the steepest descent (max force < 1000 kJ / mol / nm). Equilibrated in 2 stages: 300 K NVT ensemble (constant number of particles, volume and temperature) 100 ps, then 100 ps NPT ensemble (constant number of particles, pressure, temperature) 1 bar. The production period of 100 ns was run at an integration time of 2 fs. The long-range electrostatics were handled by the Particle Mesh Ewald (PME) with a 1.0 nm cutoff. Analysis of the trajectory included RMSD, RMSF, Rg, the occupancy of hydrogen bonds and the energy of protein / ligand interactions (GROMACS built-in tools), the visualization in XMGRACE.

2.5 ADMET Analysis

In silico pharmacokinetic and toxicity profiling of the lead compound was performed using two complementary platforms. SwissADME (swissadme.ch) was employed to evaluate physicochemical properties, Lipinski's rule of 5 adherence, GI, blood brain barrier (BBB), P-glycoprotein (PGP), and CYP450 inhibition. Solubility (Aqueous solubility (ESOL, Ali, and Silicos-IT), drug-ability, molecular property, in vitro ADMET, and toxicity were estimated (Lipinski, Veber, Egan, Muegge, and Ghose filters). Toxicity endpoints (hepatotoxicity, carcinogenicity, mutagenicity (Ames), and cytotoxicity) were predicted by Pro Tox-3 (tox.charite.de/protox3). The drug likeness score and skin permeation coefficient (log Kp) were determined as implemented in SwissADME.

3. RESULTS

3.1 Molecular Docking

Virtual screening of the 500+ phytocompound library against CYP19A1 identified Deserpidine as the highest-affinity compound, with a binding free energy of −10.2 kcal/mol notably more negative than the binding energy of the endogenous substrate androstenedione, indicating strong potential for competitive inhibition of the catalytic site. The top-ranked compounds from the docking screen are presented in Table 1.

Table 1. Top-ranked phytocompounds from virtual screening against CYP19A1 (PDB ID: 5JL6). Binding energies reported as kcal/mol.

Rank	Compound	Binding Energy (kcal/mol)	H-bonds	Key Residues
1	Deserpidine	−10.2	3	Arg115, Ile133, Phe134, Val370, Met374
2	Withanolide B	−10.2	0	-
3	Ecliptalbine	−10.3	1	Leu372
4	Picracin	−10.2	2	Gly439, Leu372
5	Cucurbitacin I	−10.2	0	-

Docking protocol validation by re-docking of the co-crystallized androstenedione yielded an RMSD of less than 2.0 Å relative to the crystallographic pose, confirming the reliability of the docking setup for this binding site.

3.2 Protein–Ligand Interaction Analysis

Analysis of the Deserpidine-CYP19A1 docked complex indicated that the ligand interacts with the androstenedione-binding cavity with as several hydrogen bonds and hydrophobic interactions (Figure 3). Deserpidine forms hydrogen bonds with the key active-site residues and hydrophobic interactions such as alkyl and π-alkyl interactions with residues Phe134, Val370, Met374, and Leu372 – these comprise the substrate-binding cavity and dictate androgen binding – is similar to the. interaction pattern of the native substrate

androstenedione, providing a mechanistic basis for competitive CYP19A1 inhibition by Deserpidine.

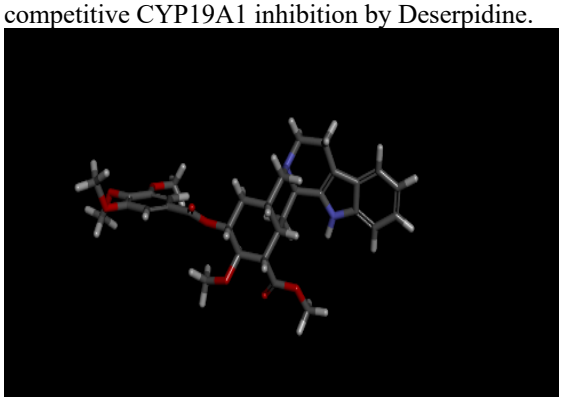


Figure 2. Two-dimensional chemical structure of Deserpidine (MW: 578.65 g/mol). Functional groups mediating active-site interactions are indicated.

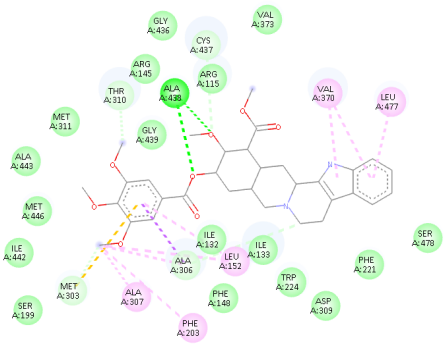


Figure 3. Two-dimensional interaction diagram of the Deserpidine–CYP19A1 docked complex. Hydrogen bond interactions are shown as green dashed lines; hydrophobic contacts (alkyl, π–alkyl) are indicated in pink.

3.3 Molecular Dynamics Simulation

3.3.1 Protein–Ligand Interaction Energy

The protein ligand interaction energy of Deserpidine binding to CYP19A1 was predominantly negative across the entire 100ns trajectory and indicates thermodynamically stable and favourable binding of all systems. Small variations in interaction energy was observed for all systems over the entire trajectory, which are typical for protein ligand interactions models in physiologically relevant simulation environments. At no point during any of the simulations was the interaction energy abruptly increased indicating ligand detachment.

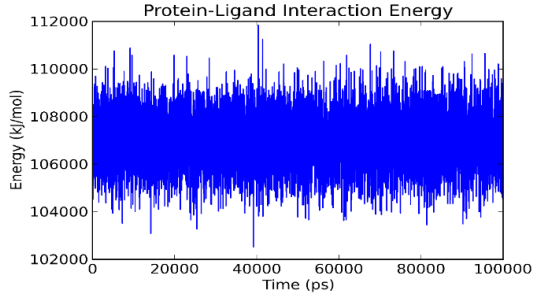


Figure 4. Protein–ligand interaction energy profile of the Deserpidine–CYP19A1 complex over the 100 ns MD simulation trajectory. Negative values throughout confirm thermodynamically stable binding.

3.3.2 Hydrogen Bond Analysis

Hydrogen bond occupancy studies indicated that the interactions between Deserpidine and the active-site residues were dynamic but stable and persisted throughout the simulation (Figure 5). During most of the simulation, one to three hydrogen bonds were formed, with notable transient occurrences of four simultaneous hydrogen bonds for the initial 25 ns. After 25 ns, the number of hydrogen bonds formed gradually decreased, as would be expected with a shift to a binding mode in which hydrophobic contacts and van der Waals interactions between Deserpidine and the steroid-binding pocket dominated the long-term stability of the complex. Such behavior is typical of enzymeinhibitor complexes and does not necessarily imply unbinding of the ligand from the binding site.

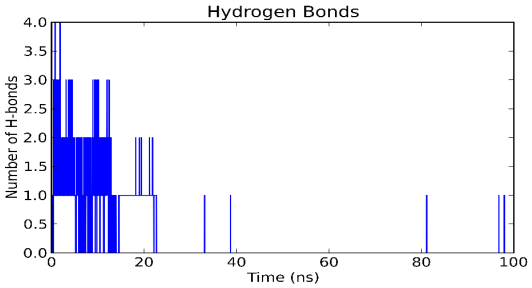


Figure 5. Hydrogen bond count between Deserpidine and CYP19A1 active-site residues over the 100 ns MD simulation. The trajectory shows 1–3 persistent hydrogen bonds throughout, with transient peaks of 4 bonds in the initial phase.

3.3.3 Radius of Gyration

The radius of gyration (Rg) of CYP19A1 remained stable between 2.27 and 2.31 nm throughout the 100 ns simulation (Figure 6), confirming that the overall compactness and globular structure of the protein were maintained upon Deserpidine binding. Rg fluctuation shows that, there was no unfolding or aggregation happened at least within the whole simulation period, which indicates the integrity of the complex kept in simulated physiological state.

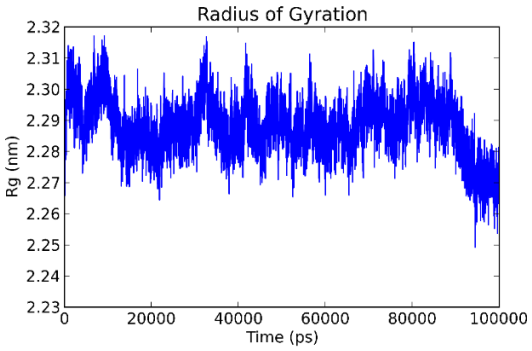


Figure 6. Radius of gyration (Rg) of the CYP19A1–Deserpidine complex over the 100 ns

MD simulation. Values remained stable between 2.27 and 2.31 nm, confirming maintained protein compactness and structural integrity.

3.3.4 RMSD Analysis

RMSD analysis Deserpidine-CYP19A1 RMSD calculated for the Deserpidine-CYP19A1 over the 100 ns trajectories showed an early slight discrepancy of ~ 10 ns, as the ligand adjusted its conformation in the active site (Figure 7). The subsequent RMSD plot showed an equilibrium of 0.22- 0.45 nm, without any continue offset from the baseline or any long-term increase for the remaining nanoseconds of the trajectory. This plateau shows the achievement of a dynamic equilibrium, confirming Deserpidine remained bound in the binding site and the complex was stable by the end of the simulation.

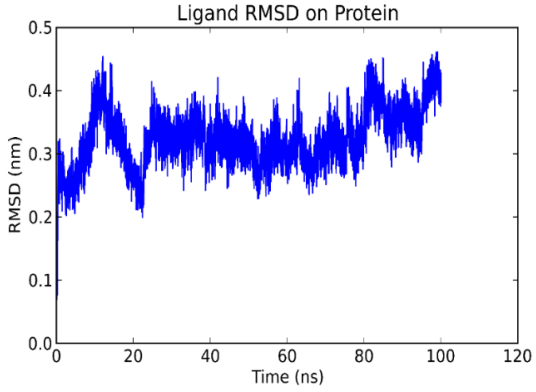


Figure 7. RMSD of the Deserpidine–CYP19A1 complex relative to the protein backbone over the 100 ns MD trajectory. After an initial 10 ns equilibration, RMSD stabilizes between 0.22 and 0.45 nm, indicating a stable protein–ligand complex.

3.3.5 RMSF Analysis

A residue-by-residue measure of flexibility (or RMSF) was obtained (Figure 8). Most amino acid residues fluctuated less than 0.20 nm, thus suggesting a very stable and rigid protein backbone upon ligand binding. Higher fluctuation values were localized to flexible protein loops and the N- and C-termini far removed from the active site. Active-site residues in direct contact with Deserpidine had high RSMF values, suggesting that ligand binding served to stabilize the protein's catalytic cavity and did not propagate further backbone motion.

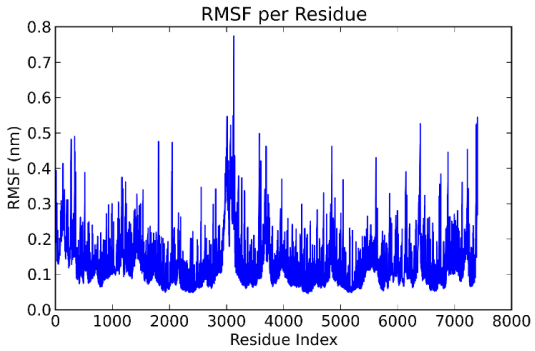


Figure 8. Root mean square fluctuation (RMSF) per residue of CYP19A1 in complex with Deserpidine. Most residues fluctuate below 0.20 nm; elevated fluctuations are restricted to terminal and loop regions distal from the active site.

3.4 ADMET Analysis

Summary of the Deserpidine ADMET profile is given in Table 2. Deserpidine (MW = 578.65 g/mol) somewhat exceeds the 500 g/mol limit of the Lipinski Rule of 5 - this is a frequent occurrence for FDA approved drugs derived from natural products and does not categorically preclude it from further development[13]. There are nine hydrogen bond acceptors and one donor, with a topological polar surface area of 108.55 Å² indicating it has the capacity to be transported across membranes, and it has moderate lipophilicity with a log P of 3.47 so it is likely to undergo passive intestinal absorption. High gastrointestinal absorption Swiss-ADME predicts the compound to be highly absorbed. Limited blood-brain barrier (BBB) permeability there is little propensity for central nervous system (CNS) related adverse reactions. The potential for inhibitory activity against CYP1A2, CYP2C19 and CYP2C9 has been flagged which accounts for some drug-drug interaction potential. These effects are experimentally determined. The molecules appear to have some interaction potential with CYP2D6 and CYP3A4. Skin permeability (log Kp = 6.92 cm/s) indicates low dermal penetration. The molecule meets Veber, Egan and Muegge drug-likeness filters. Bioavailability Score: 0.55. No mutagenic or hepatotoxic effects found with Pro Tox-3; LD50s indicate a reasonable toxicity profile.

Table 2. In silico ADMET profile of Deserpidine as predicted by Swiss ADME and ProTox-3.

Parameter	Value	Interpretation
Molecular Weight	578.65 g/mol	Marginal Ro5 exceedance; typical of natural products

Parameter	Value	Interpretation
H-bond Acceptors	9	Within acceptable range
H-bond Donors	1	Within Ro5 limit (≤5)
TPSA	108.55 Å²	Acceptable membrane permeability
log P	3.47	Moderate lipophilicity; favorable absorption
GI Absorption	High	Good oral bioavailability
BBB Penetration	Low	Reduced CNS adverse effect risk
CYP Inhibition	CYP1A2, 2C19, 2C9	Drug–drug interaction potential; evaluate experimentally
Bioavailability Score	0.55	Suitable for oral delivery
Hepatotoxicity	Inactive	Favorable
Mutagenicity (Ames)	Inactive	Favorable
log Kp (skin)	−6.92 cm/s	Low dermal penetration

4. DISCUSSION

This study presents a comprehensive in silico screening of plant-based compounds targeting the validated enzyme target of CYP19A1 in PCOD. Out of over 500 phytocompounds screened, Deserpidine was found to be the promising lead compound for CYP19A1 inhibitory activity with binding free energy of 10.2 kcal/mol - the highest binding free energy for binding energy and the complex was stable over 100 ns MD simulation. The binding orientation of Deserpidine in the active site is of direct mechanistic significance. Residues in the androstenedione-binding pocket of CYP19A1 that interact with Deserpidine - Arg115, Ile133, Phe134, Val370, and Met374 - are well-characterized as critical determinants of aromatase active-site architecture, substrate specificity, and catalysis[4]. Competitive occupation of this pocket by Deserpidine may sterically block androstenedione access directly, and thus inhibit aromatase activity (and serum estrogen levels), and reduce the formation of new excess androgen, the abnormal presence of which causes the hormonal symptoms of PCOD. Our MD simulations significantly strengthen the docking studies. The stable RMSD profile (0.22-0.45 nm after equilibration), low RMSF at the active-site residues, and constant Rg values, evidence that Deserpidine doesn't destabilize or cause disconcerting conformational changes in the CYP19A1-enzyme, while forming a structurally stable inhibitor complex that should not dissipate in vivo - another hallmark of an inhibitor with in vivo activity. The dynamic hydrogen bond profile, evolving from a polar-dominant to a hydrophobic-dominant state after 25 ns, points to a realistic adaptive binding mode for an enzyme/inhibitor interaction with high conformational pliancy. The ADMET properties of Deserpidine are generally favorable for advancement of the molecule as a lead candidate. The predicted high GI absorption and bioavailability score of 0.55 strongly favor orally delivered drugs. The single property slightly outside the Lipinski limit on molecular weight is a common issue among natural product leads that has not been a barrier to clinical development of similar molecules[13]. However, as a member of the Rauwolfia alkaloids, Deserpidine bears structural resemblance to reserpine, which has been reported to induce depression, sedation, and orthostatic hypotension due to monoamine depletion when used at therapeutic doses[14]. This monoamedepressant liability will need to be empirically studied in upcoming safety pharmacology screens and, if necessary, remedied through structural modification to separate the CYP19A1 inhibitory activity from monoamine transporter activity. These data add to the existing literature validating the potential use of phytochemicals as aromatase modulators. Flavonoids such as apigenin and quercetin have already been shown to exhibit CYP19A1 inhibitory activity using in silico and enzymatic assays[6,7]. The tetracyclic indole alkaloid structure of Deserpidine adds to the array of structurally different chemical scaffolds, exemplified by natural products, that can be pursued for the development of aromatase inhibitors. This study has several limitations. The

whole work is based on a computational pipeline that needs verification of results through aromatase enzyme activity assays, cell-based assays with granulosa cell lines and verification in vivo with PCOD animal models. A comprehensive phytocompound library is used but does not include all plant chemical space, potential future campaigns can be extended to other databases, such ZINC22, or COCONUT.

5. CONCLUSION

This in silico study identifies Deserpidine, a plant-derived indole alkaloid, as a potent candidate inhibitor of human placental aromatase CYP19A1 for the management of PCOD. Through molecular docking screening of a library of >500 phytocompounds, Deserpidine exhibited the greatest binding energy (−10.2 kcal/mol) with reliable binding energy within the androstenedione-binding pocket through hydrophobic and hydrogen bonds. Molecular dynamics simulation of the Deserpidine CYP19A1 complex demonstrated structural stability, while in silico ADMET analysis reveals overall good pharmacokinetic and safety parameters. As a class of Rauwolfia alkaloids has monoaminergic pharmacology, possible side effects need to be experimentally determined and the ligand–receptor structure optimized for laboratory evidence. In conclusion, our work provides a compelling rational basis for target-based activity screening of Deserpidine as an aromatase inhibitor for further in vitro testing and in vivo validation as a natural-product-derived treatment for PCOD.

DATA AVAILABILITY STATEMENT

The datasets supporting the conclusions of this article are included within the article.

ACKNOWLEDGMENTS

The authors thank the lab facilities provided by Kalaignarkarunanidhi Institute of Technology.

REFERENCES

[1] Devade O, Londhe RD, Sokate NV, Randave UR, Ranpise PA. A review on polycystic ovarian disorder. Asian J Res Pharm Sci. 2022;12:219–226. https://doi.org/10.52711/2231-5659.2022.00039

[2] Gadage V, Dhute R, Choukhande P, Dalvi A, Dhamne S. A review on PCOD: polycystic ovarian disease. Int J Adv Res Sci Commun Technol. 2024;4:372–379. https://doi.org/10.48175/IJARSCT-17858

[3] Rani R, Hajam YA, Kumar R, Bhat RA, Rai S, Rather MA. A landscape analysis of the potential role of polyphenols for the treatment of polycystic ovarian syndrome (PCOS). Phytomedicine Plus. 2022;2(1):100161. https://doi.org/10.1016/j.phyplu.2021.100161

[4] Ghosh D, Egbuta C, Kanyo JE, Lam TT. Phosphorylation of human placental aromatase CYP19A1. Biochem J. 2019;476(21):3313–3331. https://doi.org/10.1042/BCJ20190633

[5] Acar S, Böber E, Olguner M, Özer E, Abacı A, Özhan B, et al. A novel compound heterozygous variant in CYP19A1 resulting in aromatase deficiency with normal ovarian tissue. Turk J Pediatr. 2020;62(5):826–830. https://doi.org/10.24953/turkjped.2020.05.015

[6] Pillalamarri Madhavi PM, et al. A comparative review of herbal medicinal plants and synthetic drugs in the treatment of polycystic ovarian syndrome (PCOS). Int J Pharm Res Appl. 2025;10(1):175–183. https://doi.org/10.35629/4494-1001175183

[7] N P S. Botanical interventions for PCOS: a phytochemical perspective. Afr J Biomed Res. 2024;27(4S):14811–14816. https://doi.org/10.53555/AJBR.v27i4S.7424

[8] Nampoothiri L, Maharjan R, Dey A. Implication of non-polar phytocomponents of aloe vera gel in management of polycystic ovarian syndrome. Endocr Abstr. 2015;37:EP140. https://doi.org/10.1530/endoabs.37.EP140

[9] Masilamani SD, Hari R, Kannaiyram G, Chokkalingam P. Asparagus racemosus – a potential PCOD healer through the management of hyperglycaemia and hyperandrogenism: an in vitro and in silico approach. Res J Pharm Technol. 2023:2096–2102. https://doi.org/10.52711/0974-360X.2023.00344

[10] Liu Y, Jiang J, Du S, et al. Artemisinins ameliorate polycystic ovarian syndrome by mediating LONP1–CYP11A1 interaction. Science. 2024;384(6701):eadk5382. https://doi.org/10.1126/science.adk5382

[11] Karanovic J, Raković A. Inositol – a natural treatment for polycystic ovarian syndrome? Acta Med Int. 2016;3(1):6. https://doi.org/10.5530/ami.2016.1.3

[12] Kumar P, Deepak D, Saini V, Annu A, Yadav N, Kumar A. In silico identification of target fetal protein(s) in the development of polycystic ovarian syndrome. J Appl Biol Biotechnol. 2022;10:176–185. https://doi.org/10.7324/JABB.2022.100522

[13] Lipinski CA. Lead- and drug-like compounds: the rule-of-five revolution. Drug Discov Today Technol. 2004;1(4):337–341.

[14] Kamathenu UK, Velayudhan A, Krishna KV, Nithya R. Social anxiety and interpersonal relationship of women with PCOD. Medico Legal Update. 2021;21(3):523–528. https://doi.org/10.37506/mlu.v21i3.3040

[15] Shetye SM, Bhoir RS, Chavan SS. The herbal approach to PCOD: efficacy, safety, and future directions. Asian J Pharm Res Dev. 2025;13(3):97–104. https://doi.org/10.22270/ajprd.v13i3.1561